

Molecular analysis of the membrane insertion domain of proteinase 3, the Wegener's autoantigen, in RBL cells: implication for its pathogenic activity

Chahrazade Kantari,^{*,†} Arnaud Millet,^{*,†} Julie Gabillet,^{*,†} Eric Hajjar,[‡] Torben Broemstrup,[‡] Paula Pluta,[‡] Nathalie Reuter,^{‡,§} and Véronique Witko-Sarsat^{*,†,1}

^{*}INSERM U1016, Institut Cochin, Paris, France; [†]CNRS-UMR 8104, Université Paris Descartes, Sorbonne Paris Cité, Paris, France; [‡]Computational Biology Unit, uniBCCS, uniResearch, Bergen, Norway; and [§]Department of Molecular Biology, University of Bergen, Bergen, Norway

RECEIVED DECEMBER 20, 2010; REVISED JULY 13, 2011; ACCEPTED JULY 14, 2011. DOI: 10.1189/jlb.1210695

ABSTRACT

PR3, also called myeloblastin, is a neutrophil serine protease that promotes myeloid cell proliferation by cleaving the cyclin-dependent kinase inhibitor p21^{cip1/waf1}. In addition, it is the target of ANCA in GPA, a necrotizing vasculitis. Anti-PR3 ANCA binding to membrane-expressed PR3 triggers neutrophil activation, potentiating vascular inflammation. This study performed in RBL cells identifies the structural motifs of PR3 membrane anchorage and examines its impact on PR3 proinflammatory and proliferative functions. With the use of MD simulations and mutagenesis, we demonstrate that the mutations of four hydrophobic (F180, F181, L228, F229) or four basic (R193, R194, K195, R227) amino acids abrogated PR3 membrane anchorage. The hydrophobic patch-deficient PR3 mutant (PR34H4A) was still able to cleave the synthetic substrate Boc-Ala-Pro-Val in cell lysates. However, in contrast to WT PR3, PR34H4A was not expressed at the plasma membrane after degranulation and failed to cleave extracellular fibronectin, was not externalized after apoptosis and did not impair macrophage phagocytosis of apoptotic cells, did not promote myeloid cell proliferation and failed to cleave p21/waf1. PR3 membrane insertion appears to be pivotal for its proinflammatory activities, such as extracellular proteolysis and impairment of apoptotic cell clearance, but also for myeloid cell proliferation. Targeting membrane-associated PR3 might constitute a novel, anti-inflammatory therapeutic strategy in inflammatory disease especially in vasculitis, but this approach has to be validated in mature neutrophils. *J. Leukoc. Biol.* 90: 941–950; 2011.

Abbreviations: 7-AAD=7-aminoactinomycin D, ANCA=antineutrophil cytoplasmic antibody, FL2/3=fluorescence 2/3, GPA=granulomatosis with polyangiitis, IBS=interfacial binding site, MD=molecular dynamics, MFI=mean fluorescence intensity, PR3=proteinase 3, RBL=rat basophil cell line

The online version of this paper, found at www.jleukbio.org, includes supplemental information.

Introduction

Neutrophil-derived serine proteinases participate efficiently in the antibacterial defense [1], but they are also considered as proinflammatory proteins implicated in tissue damage during inflammatory disorders, such as emphysema, rheumatoid arthritis, and vasculitis [2]. Serine proteinase activities are controlled by physiological inhibitors, but it has been reported that membrane-associated proteinases can circumvent the effect of extracellular inhibitors and preserve their degradative capacities [3, 4]. PR3 is a neutrophil serine protease and like its homologues cathepsin G and elastase, is stored mainly in azurophilic granules [5]. However, in contrast to neutrophil elastase, PR3 localization is not solely restricted to azurophilic granules but rather, is localized at the plasma membrane in resting neutrophils and in secretory vesicles [6]. Despite the close homology between elastase and PR3, there are structural differences [7] that can explain their different affinity for the membrane and their subcellular localization. Using PR3 cDNA stably transfected mast cell lines, we demonstrated that PR3 was expressed at the cell surface after ionophore-induced degranulation. In contrast, elastase, a soluble serine-proteinase [8], was released into the extracellular medium, strongly suggesting that PR3 has sequences that allow its membrane insertion.

PR3 membrane expression is of specific relevance in GPA, formerly known as Wegener's granulomatosis, a systemic necrotizing vasculitis of unknown etiology involving the upper airways, lungs, and kidneys [9, 10]. In this disease, ANCA are directed against PR3. In turn, these anti-PR3 ANCA are thought to bind to membrane PR3 to activate neutrophils to trigger radical oxygen species generation [11], thus amplifying inflammation further. PR3 membrane expression could be enhanced by inflammatory stimuli such as TNF- α [12] or during apoptosis [13]. Notably, apoptosis-induced PR3 membrane ex-

1. Correspondence: INSERM U1016, Institut Cochin, 27 rue du faubourg St Jacques, 75014 Paris, France. E-mail: veronique.witko@inserm.fr

pression impaired the phagocytosis of apoptotic neutrophils by macrophages, thus acting as a “don’t-eat-me” signal, independently of its enzymatic activity, to potentiate inflammation and likely autoimmunity [13]. Moreover, PR3, also called myeloblastin [14], has been cloned as a serine proteinase down-regulated during myeloid differentiation and overexpressed in leukemic cells [15]. We provided evidence that PR3 had a proliferative activity as a result of the cleavage of the cyclin-dependent kinase inhibitor p21^{cip1/waf1} [16, 17]. However, whether PR3 membrane association was required for its proliferative activity was currently unknown.

PR3 does not contain a transmembrane domain and thus, can be considered as a peripheral membrane protein that can have direct interaction with lipids [18]. To investigate the molecular mechanisms involved in the association of PR3 with the plasma membrane, we previously performed molecular modeling analysis using an implicit model of the membrane [19]. Using this model, combined with calculations based on atomistic models, we were able to highlight the importance of two amino acid clusters, one charged and one hydrophobic, which may have been involved in PR3 membrane association. We also proposed that it had a unique IBS and that only a few residues of PR3 account for the membrane anchorage. Interactions among basic residues (R193, R194, K195, R227) at the PR3 surface with the membrane provides the driving force to orient PR3, enabling the hydrophobic residues (F180, F181, L228, F229) to anchor into the hydrophobic core of the membrane.

The aim of the present study, therefore, was to demonstrate that the IBS mediates PR3 membrane insertion and to examine its impact on PR3 biological functions. To this aim, we engineered point mutations in the PR3 membrane insertion domain and studied the role of PR3 membrane expression on the extracellular fibronectin degradation, on the phagocytosis of apoptotic PR3-expressing cells by macrophages, and on its p21/waf1-dependent proliferative activity.

MATERIALS AND METHODS

Molecular modeling

MD simulations with an implicit membrane model. Initial coordinates for all simulations were taken from the X-ray structure of human PR3 (Protein Data Bank ID: 1FUJ, chain A) [20]. The procedure is similar to what was described previously [19]. Briefly, we built six different orientations of PR3 with respect to the membrane, and each of them was used as the starting conformation of six independent MD simulations that use a 50% anionic bilayer. PR3 numbering conventions are used in the present study.

MD simulations of the p21^{cip1/waf1} peptide bound to WT PR3 and the PR34H4A mutant. To investigate how well the region containing the proposed cleavage site of p21^{waf1} interacts with PR3, we performed MD simulations of a complex between PR3 and a peptide mimicking the cleaved region of p21 (“IQEARER”) as described previously [17]. Briefly, the trajectories collected during the sampling time were submitted to qualitative and quantitative analysis, including a visual inspection of the trajectories and average structures and calculation of lifetime hydrogen bonds and hydrophobic interactions, respectively. The hydrophobic mutant PR34H4A was built by removing the side-chains of F180, F181, L228, and F229 and building instead, alanine side-chains. The procedures used for the system setup and the simulations are described in ref. [21].

Expression of PR3 mutants in RBL

Human rPR3 was stably expressed in RBL cells after stable transfection with pcDNA3/PR3, as described previously [16]. PR3 mutants were obtained by site-directed mutagenesis on pcDNA3/PR3 using the Quickchange method (Stratagene, La Jolla, CA, USA) and were sequenced. RBL cells were transfected using the Amaxa system, as indicated by the manufacturer. Briefly, cells (2×10^6) were resuspended in 100 μ l cell-line solution number kit T in the presence of 5 μ g plasmid (control pcDNA3/zeocin or pcDNA3/PR3). Cells were electroporated at the indicated voltage and transferred into culture plates. Transfected cells were selected and cloned on the basis on their resistance to zeocin (0.1 μ g/ml).

PR3 immunofluorescence labeling in RBL cells

RBL cells were cytospinned, fixed in PBS-4% paraformaldehyde, and permeabilized with methanol as described [13]. After saturation with PBS-1% BSA, RBL cells were incubated with the mouse anti-PR3 mAb (4A5 clone, Wieslab, Lund, Sweden), followed by an Alexa 448-conjugated antimouse IgG (Dako, Denmark). Slides were mounted using Fluoprep (Biomérieux, France) and analyzed by fluorescence microscopy using a Zeiss LSM-5 microscope.

Flow cytometry analysis of intracellular PR3 and PR3 membrane expression

Quantification of PR3 intracellular expression was performed after cell permeabilization using anti-PR3 mouse mAb (2 μ g/ml, 4A5 clone, Wieslab; or 2 μ g/ml, CLB12.8, Sanquin, Amsterdam). PR3 membrane expression was quantified by immunolabeling without permeabilization as described previously [8]. RBL were first incubated with heat-aggregated goat IgG-5% FCS to block membrane FcRs. RBL cells were next incubated for 30 min with a control IgG or the mouse anti-PR3 mAb (2 μ g/ml), followed by FITC-conjugated anti-mouse IgG (Immunotech, France) for 30 min. Cells were analyzed using a FACScan flow cytometer (CellQuest software, Becton Dickinson Immunocytometry Systems, San Jose, CA, USA).

Measurement of soluble and membrane-associated PR3 in RBL-PR3 and RBL-PR34H4A

Ionophore A23187 stimulates secretory granule exocytosis and triggers soluble PR3 extracellular release and PR3 surface expression as described previously [16]. RBL cells (2.5 or 5×10^6 cells/100 μ l) were seeded in a six-well plate and stimulated with 2 μ M A23187 ionophore (Calbiochem, San Diego, CA, USA) in HBSS, supplemented with 1.2 mM CaCl₂ for 30 min, as described previously [11]. Cell supernatants were collected and centrifuged to obtain the fraction containing the extracellular release of soluble PR3 to be detected by Western blot analysis using a rabbit polyclonal anti-PR3 as a primary antibody, as described previously [16]. To analyze the amount of membrane-associated PR3 in RBL cells, cells were disrupted by sonication to avoid the use of a detergent. This lysate was next centrifuged to obtain a pellet corresponding to the membrane-associated fraction. After washing this pellet with HBSS, supplemented with 200 mM NaCl to remove charge-bound proteins, proteins were solubilized in 100 μ l Laemmli sample buffer, and membrane-associated PR3 was analyzed by Western blot within this fraction.

Degranulation-induced PR3 membrane expression

PR3 surface expression was measured by flow cytometry under basal conditions or after stimulation with the calcium ionophore A23187, as described previously [8]. Briefly, RBL cells (5×10^5 cells/500 μ l) were incubated in HBSS, supplemented with 1.2 mM CaCl₂ for 30 min in the presence of 2 μ M A23187 ionophore to induce degranulation and were then washed with PBS. The percentage of cells expressing membrane PR3 was determined by flow cytometry after membrane PR3 immunolabeling. Degranulation was evaluated by measuring β -hexosaminidase activity in supernatant of degranulation, using the chromogenic substrate *p*-nitrophenyl-*N*-acetyl- β -D-glucosaminide.

saminide (Sigma-Aldrich, St. Louis, MO, USA), as described previously [8]. For each type of RBL cells, 50 μ l of the degranulation medium containing β -hexosaminidase and 50 μ l of the substrate (2 mM *p*-nitrophenyl-*N*-acetyl- β -D-glucosaminide in 0.2 M citrate buffer, pH 4.5) were incubated at 37°C in 96-well plates. After 1 h, 40 μ l of this reaction mixture was added to 210 μ l 0.2 M carbonate-bicarbonate buffer (pH 10) to stop the reaction, and absorbance at 405 nm was measured. Analysis was performed in triplicate. Results were expressed as a percentage of β -hexosaminidase release relative to the total intracellular content obtained after lysis of 5×10^5 cells in 500 μ l HBSS containing 1% Triton X-100 during 10 min at 4°C.

Apoptosis induction

Apoptosis was induced by incubating RBL cells (10^6 /ml) for 16 h at 37°C with 2 μ g/ml gliotoxin (Sigma-Aldrich), which is a fungal metabolite and by its direct binding to the proapoptotic protein Bak, triggers apoptosis via the mitochondrial pathway [22]. Apoptosis-induced phosphatidylserine externalization was quantified by PE-annexin-V (FL2) labeling [13], after necrotic 7-AAD-labeled cells (FL3) were excluded from the analysis using a FACScan flow cytometer (CellQuest software, Becton Dickinson Immunocytometry Systems).

PR3 enzymatic activity measurement

For the hydrolysis of Boc-Ala-Pro-Nva-SBzl, RBL cells were lysed in PBS–1% Nonidet P-40 (100×10^6 cells/ml) and centrifuged at 10,000 g for 15 min. Protein concentrations were adjusted at 0.5 mg/ml. The enzymatic activity of each cell lysate was evaluated by measuring the hydrolysis of Boc-Ala-Pro-Nva-SBzl (Sigma-Aldrich) in the presence of 5,5'-dithiobis-2-nitrobenzoic acid after 1 h incubation at 37°C, as described previously [23]. Results were expressed as OD at 405 nm. For the cleavage of fibronectin, which is one of the major components of the ECM that has been shown to be cleaved by PR3 [4, 5], RBL cells (5×10^5 cells/ml) were stimulated with 2 μ M A23187 ionophore for 30 min to trigger degranulation, resulting in the release of soluble, granular PR3 and the expression of membrane-associated PR3. To assess the proteolytic activity of soluble proteases, the supernatant was collected and incubated with fibronectin (Calbiochem) at 50 μ g/100 μ l at 37°C for 3 h. They were next analyzed on a 12.5% SDS-PAGE, followed by silver staining to visualize fibronectin cleavage products. To evaluate the enzymatic activity of membrane-bound proteases, the ionophore-stimulated RBL cells were washed once with PBS supplemented with NaCl 400 mM to eliminate soluble and charged-bound PR3, and twice in PBS. RBL cells were incubated 3 h with purified human fibronectin 50 μ g/100 μ l at 37°C. Cells were pelleted and discarded. The supernatants containing fibronectin fragments cleaved by membrane proteinases were collected and analyzed on a 12.5% SDS-PAGE, followed by silver (to compare with soluble proteases) or Coomassie blue staining (to compare the activities of membrane-bound proteases in different RBL cell transfectants) to visualize fibronectin cleavage products. When indicated, α 1-antitrypsin (Calbiochem) was used at 5.4 μ M.

Quantification of phagocytosis of apoptotic RBL by macrophages

Human monocytes were isolated from blood with Ficoll and plated in IMDM in 12-well plates. After 1 h, nonadherent cells were removed, and cells were cultured in IMDM with 10% of autologous serum. The phagocytosis assay was performed on Day 7. Control and apoptotic RBL cells were loaded with 50 μ g/ml TAMRA (Molecular Probes, Eugene, OR, USA) during 1 h. TAMRA-loaded RBL cells (10^6 ; red fluorescence) were incubated with 10^6 macrophages for 2 h at 37°C. After two washes with PBS, cells were detached from the plates, labeled with FITC-conjugated anti-CD14 antibody (Immunotech), fixed, and deposited on poly-L-lysine-coated slides as described previously [13]. Phagocytosis was analyzed by counting under the fluorescence microscope (Leica DMI6000) the number of CD14⁺ macrophages that has ingested a TAMRA-loaded apoptotic RBL cell. A minimum of 200 CD14⁺ cells was counted for each slide by two blinded investigators.

Measurement of RBL cell proliferation and p21^{cip1/waf1} Western blot analysis

RBL cell proliferation was measured after BrdU incorporation and immunodetection (Merck, Rahway, NJ, USA). RBL cell lysates were subjected to Western blot analysis, as described previously [16]. The primary antibody was a rabbit polyclonal anti-p21 (Santa Cruz Biotechnology, Santa Cruz, CA, USA). The membrane was stripped in Restore buffer solution (Pierce, Rockford, IL, USA) and reprobed with a mouse anti- β -actin mAb (Sigma-Aldrich) as loading control.

Statistical analysis

Statistical analysis was performed using the Statview software package (SAS Institute, Cary, NC, USA). Comparisons were made using the nonparametric Mann-Whitney test or the Student's *t* test when appropriate.

Online Supplemental material

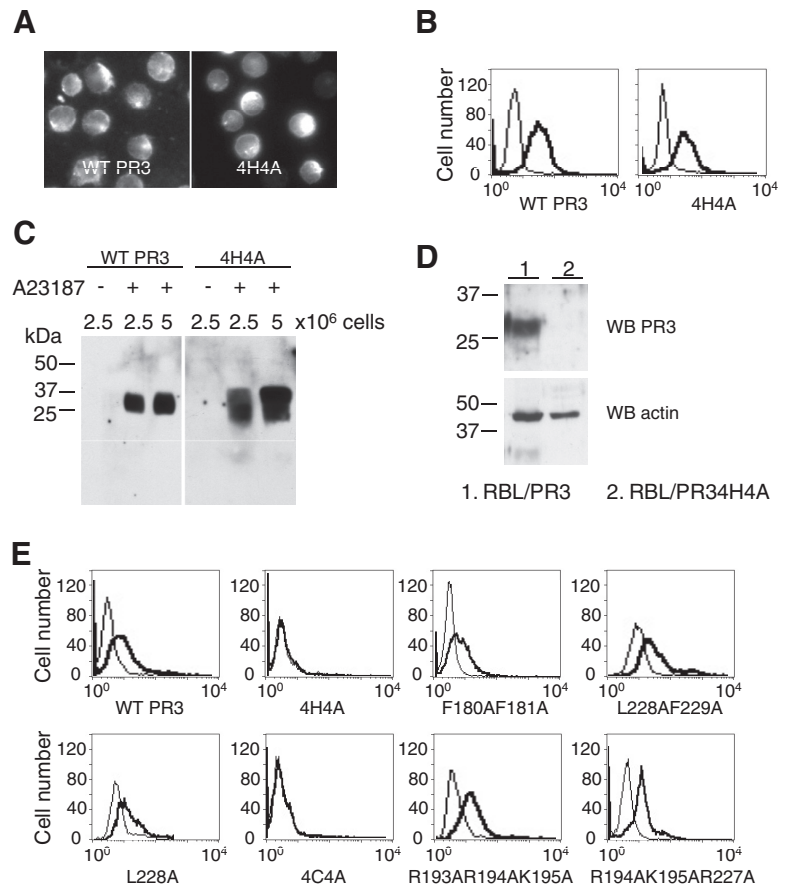
Supplemental Table 1 shows the analysis by MD simulation of the hydrogen bonds between the amino acids of the catalytic triad after docking of the p21 peptide in WT PR3 and in the hydrophobic patch-deficient mutant PR34H4A. Supplemental Fig. 1 shows the expression of membrane PR3 restricted to annexin-V⁺ cells after gliotoxin-induced apoptosis. Supplemental Fig. 2 shows the absence of effect of trypsin pretreatment on PR3 membrane expression. Supplemental Fig. 3 confirms the lack of cross-reaction between two commercial anti-human CD177/NB1 antibodies and rat CD177 expressed in RBL cells.

RESULTS

The hydrophobic patch F180-F181-L228-F229 is essential for PR3 membrane anchorage

PR3 mutants were stably expressed into RBL cells to evaluate the respective importance of the hydrophobic and the charged clusters on PR3 membrane expression after degranulation. Fluorescence microscopy analysis of PR34H4A mutants, in which the four hydrophobic amino acids F180, F181, L228, and F229 were mutated into alanine, shows similar intracellular localization between PR34H4A and WT PR3 for each cell (Fig. 1A). Flow cytometric analysis of permeabilized RBL cells showed that intracellular PR3 was expressed in >95% of RBL cells transfected with WT or mutant PR3 plasmids (Fig. 1B). The amount of intracellular PR3 was similar, as no significant difference was found in the MFI between RBL-PR3 and RBL-PR34H4A (Fig. 1B). Next, RBL cells were stimulated with A23187 ionophore to trigger the extracellular release of soluble PR3 (Fig. 1C). In the absence of ionophore, no PR3 could be detected within the supernatant in RBL-PR3 or in RBL-PR34H4A. In contrast, in the presence of ionophore treatment, soluble PR3 could be detected in the supernatant of RBL-PR3 by Western blot analysis. Furthermore, as the number of stimulated RBL cells increased, so did the amount of soluble PR3 released. Notably, the amount of soluble PR3 released into the supernatant was greater in the case of RBL-PR34H4A as compared with RBL-PR3. Accordingly, PR3, within the membrane-associated fraction, was undetectable in RBL-PR34H4A, whereas it was present in WT RBL-PR3 (Fig. 1D). These data show that PR34H4A was released more readily as a soluble protein upon cell stimulation, strongly suggesting that it was not associated with membrane.

Figure 1. Expression of PR3 mutants in RBL cells and evaluation of PR3 membrane expression after ionophore A23187 stimulation. (A) Fluorescence microscopy analysis of PR3 immunolabeling in permeabilized RBL-PR3 (WT PR3) or RBL-PR34H4A (4H4A). (B) Flow cytometric analysis of intracellular PR3 expression in permeabilized RBL-PR3 or RBL-PR34H4A. The percentages of PR3-expressing cells were 96% and 97% for RBL-PR3 and RBL-PR34H4A, respectively. (A and B) The data show the PR34H4A mutant, but identical results were obtained with all of the PR3 mutants studied. (C) Western blot analysis of soluble PR3 released into the supernatant of ionophore-stimulated RBL cells. RBL-PR3 or RBL-PR34H4A cells were seeded at 2.5 or 5×10^6 cells/well in the absence (–) or in the presence (+) of $2 \mu\text{M}$ A23187 ionophore. Western blot analysis was performed using a rabbit polyclonal anti-PR3 as primary antibody. All of the samples have been run on the same gel, and scanned membrane has been cut for clarity of the figure. (D) Western blot (WB) analysis of PR3 within the membrane-associated fraction of RBL cells after ionophore stimulation. Each well was loaded with 2.5×10^6 cells, and Western blot analysis was performed as in C. Western blot analysis of β -actin was used as control loading. (E) Flow cytometry analysis of PR3 membrane expression after ionophore-induced degranulation in RBL cells expressing the different hydrophobic (upper panels) or charged mutants (4H4A means F180AF181AL228AF229A and 4C4A means R193AR194AK195AR227A). All panels showed a representative experiment out of (at least) four, leading to similar results.



Next, PR3 membrane expression was determined by flow cytometry, before and after A23187 ionophore-induced degranulation. As described previously [8], no membrane PR3 could be detected on the RBL/PR3 cell surface under basal conditions (data not shown). As expected, the A23187 ionophore induced PR3 membrane expression in RBL-PR3. In contrast, no PR3 was expressed at the membrane of RBL-PR34H4A, thus demonstrating that the hydrophobic patch composed of the hydrophobic residues F180-F181-L228-F229 was essential for PR3 membrane anchorage (Fig. 1E). However, RBL-expressing PR3, mutated in one (PR3L228A), two (PR3F180A-F181A), or (PR3L228A-F229A) or even three (PR3F180A-L228A-F229A) of the hydrophobic residues, was still able to display membrane PR3 after degranulation (Fig. 1E and Table 1). Of note, all hydrophobic PR3 mutants, except PR34H4A, expressed membrane PR3 with the same fluorescence intensity as the WT PR3. Interestingly, PR3L228A containing a single point mutation on L228, which was predicted to make the strongest contribution to the membrane-binding affinity [21], was also membrane-associated. This indicates that the four hydrophobic amino acids cooperate for an optimum insertion, and mutations of all four are necessary to abrogate PR3 membrane anchorage.

To further validate the relevance of our MD simulation with an implicit membrane model, we performed six MD simulations for each hydrophobic mutant, each of them starting with a different orientation of the protein with re-

spect to the membrane [19]. Although the six simulations of PR34H4A resulted in an orientation of PR3, where the putative IBS faces the membrane, none of them predicted an insertion (Fig. 2A), thus confirming the absence of binding to the plasma membrane observed experimentally. In addition, simulations of PR3F180A-F181A or PR3L228A-F229A mutants confirmed a membrane anchorage of these proteins.

Implication of the basic cluster R193-R194-K195-R227 in PR3 membrane insertion

We next engineered the charge-mutated PR3, so-called PR34C4A, in which R193, R194, K195, and R227 were mutated to alanine. Ionophore-induced degranulation in RBL-PR34C4A did not result in PR34C4A membrane expression, as compared with RBL-PR3, thus demonstrating that the integrity of this charged cluster was necessary for PR3 membrane expression (Fig. 1E). However, mutation of only three out of the four charged amino acids to alanines (R193, R194, and K195 or R194, K195, and R227) did not affect PR3 membrane expression. MD simulations of the PR34C4A mutant did not show any binding of PR3 to the membrane model (Fig. 2B), except if the simulation were initiated with the protein positioned so that the hydrophobic cluster already faced the membrane model. However, unlike the experimental results, when only one charged amino acid was present (R227 or R193), MD simulations predicted an absence of PR3 insertion. This combined

TABLE 1. Quantification of PR3-Expressing Cells in RBL Cells Stably Transfected with WT PR3 or PR3 Mutated within Its IBS

PR3 mutants expressed in RBL cells	Membrane PR3-expressing cells (%)	Membrane expression
WT PR3	54.4 ± 5.2 (n=18)	Yes
Mutations on PR3		
F180AF181AL228AF229A (4H4A)	0 ± 0 (n=12) ^a	No
F180AL228AF229A	59.2 ± 7.9 (n=5)	Yes
F180AF181A	46.4 ± 4.3 (n=4)	Yes
L228AF229A	43.8 ± 8.7 (n=5)	Yes
L228A	54.2 ± 4.9 (n=8)	Yes
R193AR194AK195AR227A (4C4A)	0 ± 0 (n=12) ^a	No
R193AR194AK195A	49.9 ± 8.3 (n=5)	Yes
R194AK195AR227A	57.2 ± 9.1 (n=5)	Yes

WT PR3 or PR3 mutants were stably transfected in RBL cells. Membrane PR3 expression was triggered by A23187 ionophore and was evaluated by flow cytometry analysis after PR3 immunolabeling. The data are the percentage of RBL cells expressing membrane PR3, expressed as the mean ± SEM of at least four independent experiments. ^aDifference between WT PR3 and the PR3 mutant is statistically significant using the nonparametric Mann-Witney test ($P < 0.001$).

study illustrates the predictive value and the limit of the membrane model used, especially concerning the role of individual amino acids within the charged cluster. It has been instrumental in predicting the IBS and designing mutagenesis experiments, which in turn, are necessary to understand the fine balance of amino acid contributions in PR3 membrane anchoring. Indeed, our results demonstrate the importance of the basic and hydrophobic amino acids; proper orientation is achieved, thanks to the former, whereas the latter constitutes

the motif that is inserted into the membrane hydrophobic core (Fig. 2C).

Impaired extracellular fibronectin cleavage in the absence of PR3 membrane expression

We next investigated whether PR3 biological activities might be affected in RBL-PR34H4A cells. Measurement of the PR3 enzymatic activity toward a short peptide (Boc-Ala-Pro-Val) was performed using stably transfected RBL cell lysates as described previously [8, 23]. Notably, WT PR3 and PR34H4A could cleave this substrate with similar efficiency (Fig. 3A), thus suggesting that the mutation of the four hydrophobic residues did not affect PR3 proteolytic function when measured within cell lysates. Of note, MD simulations of PR34H4A in explicit solvent show that the mutations did not affect the catalytic or the ligand-binding sites [24]. To verify that the intracellular trafficking of proteins to granules in RBL-PR3 and RBL-PR34H4A was not modified, we studied A23187 ionophore-induced β -hexosaminidase release in these two cell lines (Fig. 3B). β -Hexosaminidase release was similar in RBL-PR3 and RBL-PR34H4A, suggesting that the trafficking of granular enzymes was not affected in RBL-PR34H4A. Next, the extracellular proteolytic activities of RBL-PR3 or RBL-PR34H4A were assessed by the cleavage of the matrix protein fibronectin to evaluate the tissue damage potential of each cell line. Expression of membrane-associated proteinases was triggered by A23187-induced degranulation, as shown already in Fig. 1E. In the absence of stimulation, no PR3 membrane expression could be detected in any of the RBL cells tested: WT-RBL, RBL-PR3, or RBL-PR34H4A cells. This was consistent with a low basal fibronectin cleavage, which was roughly similar in the supernatant of all three transfectants (Fig. 3C). In contrast, after A23187-induced degranulation, more fibronectin cleavage products were detected in the supernatant of RBL-PR3 as compared with supernatants from WT-RBL or RBL-

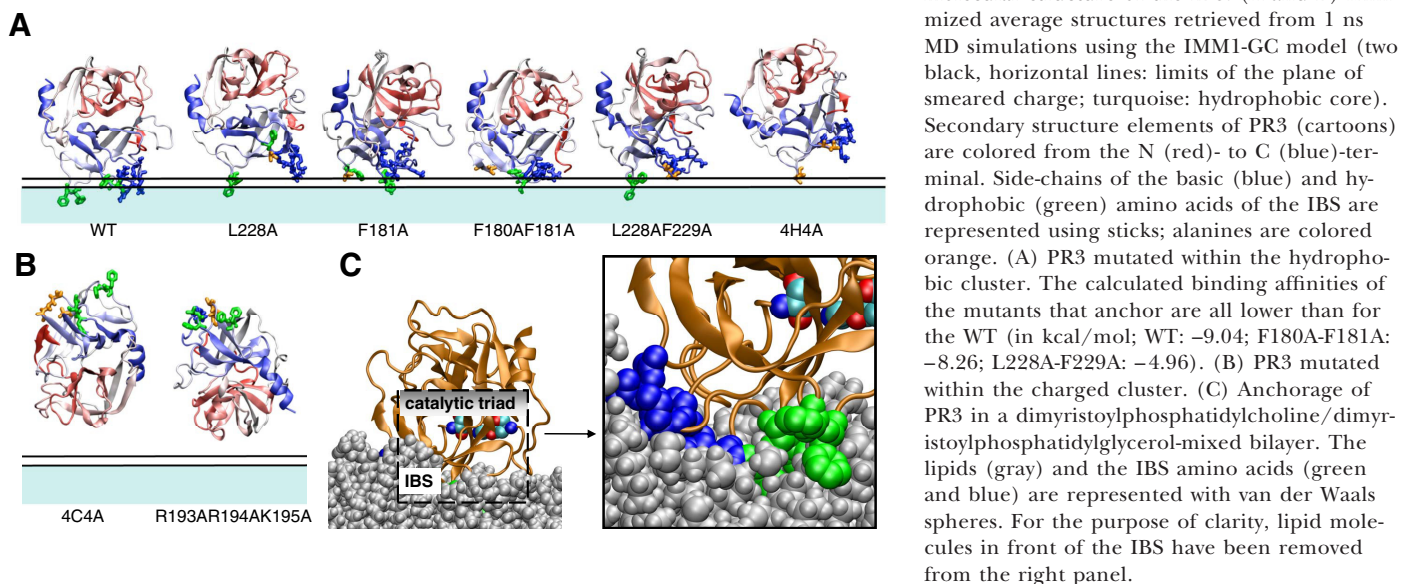
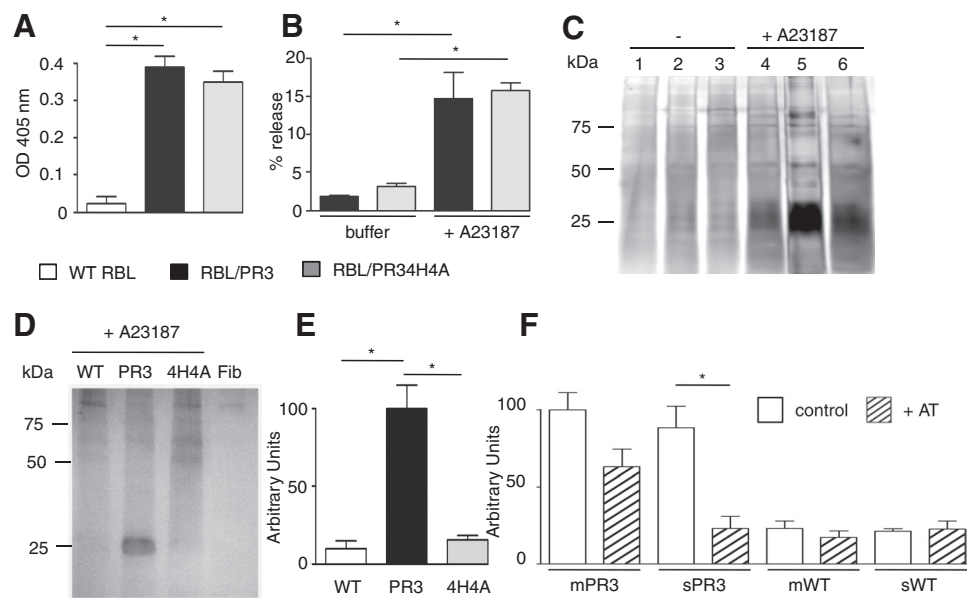


Figure 3. Evaluation of PR3 enzymatic activity in cell lysates and at the cell surface in control RBL, RBL-PR3, and RBL-PR34H4A. (A) Assessment of PR3 enzymatic activity in RBL cell lysates using the chromogenic peptide. WT-RBL, RBL-PR3, or RBL-PR34H4A was lysed, and the chromogenic peptide hydrolysis was measured by OD at 405 nm after 30 min at 37°C. Data are mean \pm SEM of four independent experiments performed in duplicate ($*P < 0.05$, Student's *t* test). (B) β -Hexosaminidase release in RBL-PR3 and RBL-PR34H4A, with or without the A23187 calcium ionophore (2 μ M) stimulation. Data are means \pm SEM from four independent experiments ($*P < 0.05$, Student's *t* test). (C) Global assessment of extracellular fibronectin cleavage in RBL cell supernatants. Untreated or A23187-treated RBL cells were incubated with soluble fibronectin for 3 h. WT-RBL (Lanes 1 and 4), RBL-PR3 (Lanes 2 and 5), or RBL-PR34H4A (Lanes 3 and 6) was pelleted, and supernatant was analyzed by SDS-PAGE, followed by silver staining to visualize all fibronectin fragments. The panel shows a representative experiment performed eight times and giving the same results. (D and E) Quantification of the intensity for the 25-kD fragment on Coomassie blue-stained gel shown in D and the histogram shown in E. Data are the relative intensities of the 25-kDa band expressed in arbitrary units, setting RBL-PR3 at 100%. Data are the mean \pm SEM from three experiments ($*P < 0.05$, Student's *t* test). (F) Effect of α 1-antitrypsin on fibronectin cleavage by membrane-associated (m) versus soluble (s) PR3. RBL cells were stimulated with A23187 as in B. Fibronectin was added to membrane-associated PR3 (as in C or D) or to the supernatant of A23187-stimulated RBL-PR3 and was used as a source of soluble PR3 in the presence or absence of α 1-antitrypsin (AT; 5.2 μ M). The membrane and the soluble fractions corresponded to 0.5×10^5 cells in this assay. Quantification of the 25-kDa fibronectin fragment was taken as a readout of fibronectin cleavage by PR3 as in E. WT-RBL cells were used as controls in these experiments. Data are the mean \pm SEM from three experiments ($*P < 0.05$, Student's *t* test).



PR34H4A and visualized on the silver-stained gel (Fig. 3C). The increased extracellular proteolytic activity was evidenced by the presence of newly generated fibronectin fragments at 25 kDa, which can be detected easily on Coomassie blue-stained gel. Quantification by densitometric scanning of this 25-kD band (Fig. 3D) showed a significant increase in extracellular proteolytic activity for RBL-PR3 as compared with RBL-PR34H4A (Fig. 3E).

To evaluate the respective importance of membrane-associated PR3 versus soluble PR3, which can be released upon degranulation in an inflammatory site, their respective sensitivity to α 1-antitrypsin, the main physiologic inhibitor of PR3 enzymatic activity, has to be taken into account [4, 5]. To do so, the inhibitory effect of α 1-antitrypsin on the extracellular fibronectin cleavage by membrane-associated versus soluble PR3 was studied. We were able to show that the inhibitory effect of α 1-antitrypsin was far greater on soluble PR3 than on membrane-bound PR3 (Fig. 3F), thus confirming previously published results [4]. From this, it is logical to infer that in a physiological setting, membrane-associated PR3 is probably the highest source of enzymatically active PR3 that can be implicated in extracellular matrix degradation.

The hydrophobic PR34H4A mutant is not externalized during apoptosis and does not display a don't-eat-me activity

As described previously, PR3 can be externalized during apoptosis in the absence of degranulation in mature neutrophils

or in RBL-PR3 [12]. So, we next examined whether the hydrophobic patch was also essential in PR3 membrane expression during apoptosis, which was induced in RBL-PR3 and RBL-PR34H4A by gliotoxin and was assessed by the increase of phosphatidylserine externalization measured by flow cytometry after PE-conjugated annexin-V labeling. In addition, labeling with 7-AAD allowed monitoring of necrosis. Negative RBL-PR3 cells under basal conditions became positive after apoptosis induction (Fig. 4A). As described previously [8, 13], double-labeling PR3 and annexin-V showed that PR3 was coexternalized with phosphatidylserine (Supplemental Fig. 1). No significant difference was found between the percentage of annexin-V-positive cells in RBL-PR3 and RBL-PR34H4A ($58.8 \pm 11.0\%$ vs. $55.6 \pm 9.6\%$, respectively; $n=10$). However, membrane PR3 was not expressed in apoptotic RBL-PR34H4A (Fig. 4A) but was strongly expressed in apoptotic RBL-PR3 (Fig. 4A), with $40.4 \pm 2.4\%$ of these cells expressing membrane PR3. This demonstrates that the hydrophobic patch was also required for PR3 membrane expression in apoptotic cells. We have shown previously that PR3 membrane expression during apoptosis impaired macrophage phagocytosis of apoptotic cells, thus acting as a don't-eat-me signal [13]. Accordingly, macrophage phagocytosis of apoptotic WT-RBL, RBL-PR3, or RBL-PR34H4A cells was studied by measuring the percentages of CD14⁺ macrophages that have ingested apoptotic TAMRA-loaded RBL cells (Fig. 4B). Notably, the level of phagocytosis by human macrophages of apoptotic RBL-PR34H4A was similar to those of WT-RBL, as RBL-PR34H4A cells lack apoptosis-induced membrane expression of PR3. In contrast and as ex-

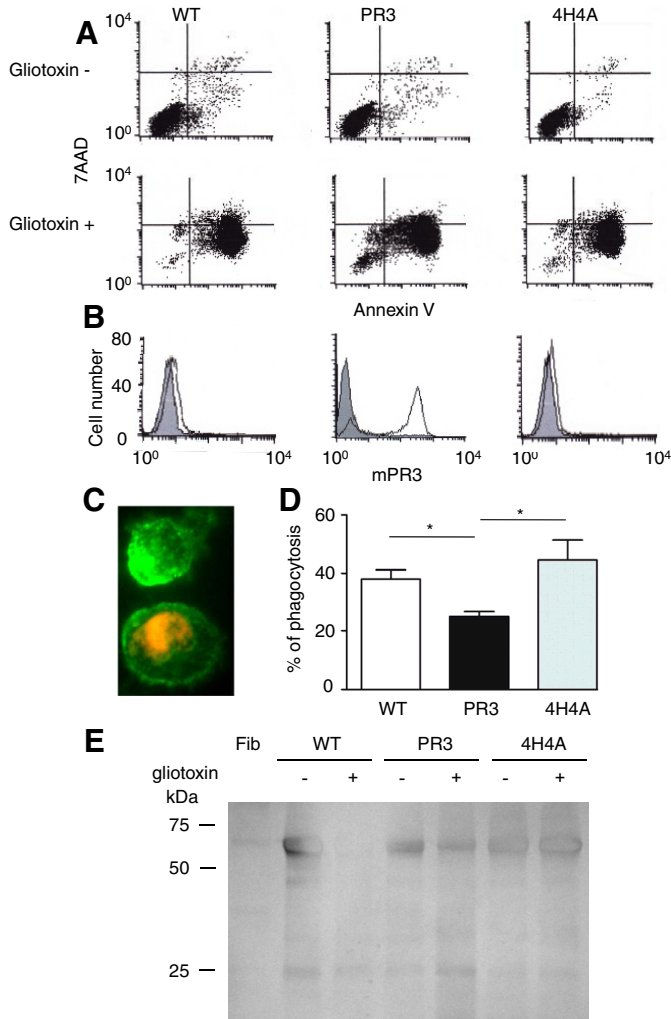


Figure 4. Apoptosis-induced PR3 membrane expression in RBL-PR3 and RBL-PR34H4A. Apoptosis was induced by gliotoxin (2 μ g/ml for 15 h) in WT-RBL, RBL-PR3, and RBL-PR34H4A. (A) Measurement of apoptosis by flow cytometry analysis of phosphatidylserine externalization by PE-conjugated annexin-V and 7-AAD labeling. (B) Measurement of PR3 membrane expression using the mouse anti-PR3 mAb (CLB12.8) compared with an isotypic-specific control antibody. The representative experiment shown here and in A has been performed 15 times with identical results. (C) Apoptotic RBL phagocytosis by human monocyte-derived macrophages after 2 h of incubation at 37°C. Macrophages are stained by anti-CD14 FITC antibodies (green), and RBL are stained by TAMRA (orange). Phagocytosis yielded a red-labeled apoptotic RBL engulfed by a green-labeled macrophage, as shown on the immune-fluorescence picture. (D) Quantification of apoptotic RBL WT, PR3, and PR3-4H4A phagocytosis. Data are means \pm sem of four independent experiments (* P < 0.05, Student's t test). (E) Assessment of fibronectin (Fib) cleavage by WT-RBL, RBL-PR3, and RBL-PR34H4A in the basal state and after gliotoxin-induced apoptosis using a 12.5% SDS-PAGE gel and silver-stained as in Fig. 3C. This representative experiment has been performed four times with identical results.

pected, RBL-PR3 cells were less phagocytosed by macrophages compared with WT-RBL or RBL-PR34H4A cells (Fig. 4C).

As gliotoxin-induced PR3 membrane expression (Fig. 4A) was significantly higher than degranulation-induced PR3 mem-

brane expression (Fig. 1E), as assessed by the MFI (394 ± 98 vs. 72 ± 9 , respectively; $n=8$; $P < 0.001$, Student's t test), we sought to evaluate its enzymatic activity by measuring extracellular fibronectin cleavage, as we did for degranulation-induced membrane PR3 in Fig. 3D. Remarkably, no fibronectin cleavage could be detected in gliotoxin-treated RBL-PR3, as only the same background fibronectin cleavage was detected for WT-RBL, RBL-PR3, and RBL-PR34H4A cells in basal or apoptotic conditions (Fig. 4D). We conclude that PR3, expressed at the membrane of apoptotic RBL-PR3 cells, is not enzymatically active but inhibited macrophage phagocytosis independently of its catalytic activity.

The hydrophobic PR34H4A mutant failed to show proliferative activity and to cleave p21^{cip1/waf1}

As described previously [16, 17], the cleavage of p21^{cip1/waf1} results in a proliferative effect in RBL-PR3. Accordingly, using BrdU incorporation, we observed that the proliferation of RBL-PR3 cells was increased significantly when compared with control RBL (Fig. 5A). In contrast, the hydrophobic mutant

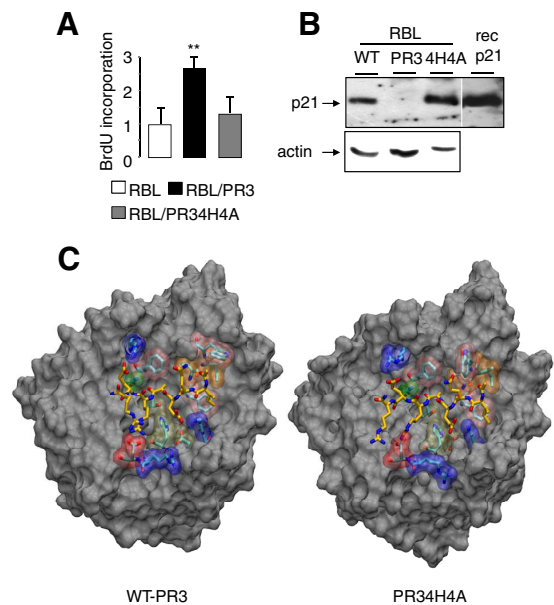


Figure 5. PR3 plasma membrane insertion in p21^{cip1/waf1} cleavage in RBL cells. (A) Measurement of RBL cell proliferation using BrdU incorporation. ** P < 0.01, Student's t test. (B) Western blot analysis was performed on RBL cell lysates (50 μ g protein/lane) either in wild type RBL (WT) or in RBL-PR3 (PR3) or in RBL-PR34H4A (PR34H4A) using a rabbit polyclonal anti-p21 antibody as primary antibody. Recombinant p21/waf1 (rccp21) produced in *Escherichia coli* was used as positive control as previously described [13] and indicate the correct molecular weight for p21. Western blot analysis of β -actin was used as control loading. (C) MD simulations of the PR34H4A mutant bound to the IQEARER p21-cleavable peptide. The solvent-accessible surfaces of the proteins are drawn in gray, and amino acids relevant for the peptide binding are colored according to their type (blue: positively charged; red: negatively charged; orange: hydrophobic; pink: aromatic; green: catalytic triad). These snapshots taken at the end of the MD simulations of WT PR3 (left) and PR34H4A (right) bound to the p21 peptide IQEARER, which appears in yellow within the catalytic triad.

PR34H4A did not show any proliferative activity, compared with the WT PR3, and its proliferation rate was similar to that of control RBL (Fig. 5A). Furthermore, Western blot analysis of p21^{cip1/waf1} expression showed that p21^{cip1/waf1} was cleaved in RBL-PR3, whereas no such cleavage was observed in RBL-PR34H4A (which shows PR3 enzymatic activity, as shown in Fig. 3A) or in control RBL (Fig. 5B). As identified previously by our lab [17, 21], the cleavage site on p21^{cip1/waf1} is at the alanine 45 residue within the peptide IQEARER, which is known to bind PR3. We next tested by MD simulations the binding capacity of our PR34H4A hydrophobic mutant to this peptide, as described previously [17, 21], to see whether the mutations within the hydrophobic cluster in PR34H4A would impair the PR3 capacity to cleave p21^{cip1/waf1}. Analysis of the simulations shows that the interaction patterns of the PR34H4A were similar to those of the WT with the IQEARER peptide and with other peptides that we investigated previously [21, 25]. Analysis of the simulations shows that the overall structure of the protein was not affected significantly by the mutations of the four amino acids into alanine. This is demonstrated by the hydrogen bond network between the amino acids of the active site similar to that observed for the WT, which itself displays the hydrogen bond network expected to be found in a Michaelis complex (Supplemental Table 1). Hence, the IQEARER peptide fits into the PR3-binding sites for the WT and the PR34H4A mutant (Fig. 5C). The structural characteristics of the PR34H4A catalytic triad indicate that this mutant retains its catalytic efficiency. Therefore, we concluded that the absence of p21^{cip1/waf1} cleavage in the RBL-PR34H4A was not a result of an inability to cleave its substrate but rather, an inability to have access to it. Remarkably, PR3 membrane association appears to play a critical role in PR3 intracellular functions, such as the control of p21^{cip1/waf1} cleavage and subsequent myeloid proliferation.

DISCUSSION

This report clearly shows that PR3 interacts with the membrane through the hydrophobic and charged clusters, which were predicted previously, and these interactions are pivotal for its proinflammatory functions. Notably, we described a novel, hydrophobic, patch-deficient PR3 mutant that might be used for functional studies to understand the importance of PR3 membrane association in its biological functions. As the mutations in the PR34H4A are on the surface and not in the protein core, the folding of the PR34H4A appears very close to those of WT PR3. The fact that PR34H4A retains its enzymatic activity confirms this view. It should be noted that the binding of peripheral proteins to membrane surfaces is critical to many biological processes and is often accomplished through lipid-interacting protein domains. This is most probably the case between PR3 and membranes. Indeed, like PR3, these proteins also require hydrophobic motifs, providing additional membrane attachment mechanism [26].

Besides the well-characterized pool of PR3 within the azurophilic granules [5], it seems that there are different pools of PR3 in neutrophils that might use different targeting mechanisms to be addressed to the plasma membrane [27]. Accord-

ing to this view, degranulation- or apoptosis-induced PR3 membrane expression appears to have different functions and different partner proteins [28]. However, we here provide evidence in RBL cells that the structural requirement for PR3 membrane anchorage is the same in both cases and is dependent strictly on the hydrophobic and charged clusters that we have identified.

In RBL cells, the molecular mechanisms involved in the degranulation- or the apoptosis-mediated PR3 membrane expression are distinct. Accordingly, the PR3 pools that are mobilized are biochemically and functionally different: ionophore-induced PR3 expression results in the membrane expression of an active protease, which was stored into secretory granules; it has a proinflammatory activity by cleaving extracellular matrix proteins or immune proteins [2]. In contrast, we have shown previously that apoptosis-induced PR3 membrane expression was independent of degranulation [13], did not trigger soluble PR3 release [8], and impaired the phagocytosis of apoptotic cells by macrophages, independently of PR3 enzymatic activity, as the inactive PR3S203A mutant showed the same activity [13]. We here provide direct evidence that membrane PR3 externalized during apoptosis was not enzymatically active, as it failed to cleave extracellular fibronectin, thus corroborating the fact that the enzymatically inactive PR3 externalized during apoptosis does not originate from the granular pool. In addition, in neutrophils, there is a "constitutive" PR3 expression at the membrane of resting neutrophils [29], which is not present on RBL-PR3 [8]. It has been suggested that this "constitutive membrane expression" was enzymatically active [30].

We concluded that in RBL cells, the PR34H4A mutant failed to be expressed at the plasma membrane and was deprived of the above-mentioned proinflammatory activities of membrane PR3, namely, the degradative capacity or the don't-eat-me activity induced, respectively, after degranulation or apoptosis.

The importance of membrane-bound PR3 in inflammatory diseases and vasculitis

We have shown previously that a high level of basal PR3 membrane expression characterizes a proinflammatory factor in vasculitis and in rheumatoid arthritis [31]. The basal PR3 expression can be enhanced greatly by inflammatory stimuli, such as TNF- α , which triggers neutrophil degranulation [6]. Our results, described in the present study in RBL cells, combined with published data [3, 4] obtained in mature neutrophils, allow the proposition that degranulation-induced membrane PR3 expression is probably the most "deleterious" form of PR3 compared with soluble PR3 released upon activation [6, 8]. Indeed soluble PR3, which should be diluted in the extracellular medium, can be inhibited by serine protease inhibitors such as α 1-antitrypsin. This latter example is a potent inhibitor of soluble PR3 [4] but as shown in the present study, is far less efficient to inhibit membrane-bound PR3. From this, it is logical to propose therapeutic strategies aiming to interfere with PR3 membrane expression as potential, new anti-inflammatory compounds. In this line of thinking, the abrogation of PR3 membrane expression would also favor the resolution of inflammation, as membrane expression dramatically decreased the phagocytosis of apoptotic cells by macrophages,

thereby perpetuating the inflammatory process and potentiating autoimmunity [27]. This potential therapeutic strategy might be specifically useful in GPA (Wegener's granulomatosis), in which the circulating anti-PR3 ANCA, which binds PR3 expressed at the membrane of activated neutrophils, might potentiate inflammation [9].

Role of the hydrophobic patch in the interactions with PR3 partners

Another feature of PR3 is its ability to associate with partner proteins, forming protein scaffolds that might be involved in PR3 membrane association and consequently, implicated in pathogenic activity [27, 28]. Notably, we observed that trypsin treatment of RBL-PR3 cells before ionophore stimulation did not modify PR3 membrane expression (Supplemental Fig. 2), thus suggesting that surface proteins do not seem to be pivotal to PR3 membrane anchorage. However, proteins expressed at the granule membrane or at the innerface of the plasma membrane, which could be externalized upon degranulation or apoptosis, could still be involved in PR3 membrane expression. The involvement of the PR3 hydrophobic patch, which we have described in mediation of protein-protein interactions, remains unknown.

Interestingly, PR3 has been shown to associate with CD177 (also called NB1), which is present only on the PR3-expressing neutrophil subset [32, 33]. It seems that CD177 is important for restriction of PR3 membrane expression to a particular subset of neutrophils [29]. It has been suggested that the hydrophobic patch, which we have defined previously as the IBS, could be involved in the PR3 association with CD177 [34], and a recent study has shown that small molecules can interfere with this association [35]. In the present study, we verify that no human CD177 was detected on the RBL cell surface using antibodies reacting with human CD177 (Supplemental Fig. 3) [32, 33], suggesting that in our cellular model, PR3 membrane expression is not dependent on CD177. Again, it should be emphasized that neutrophil-specific protein expression, which is not expressed in RBL cells, might be important in PR3 membrane expression under the basal, apoptotic, or activated state. For instance, in the RBL cell model, there is no constitutive PR3 membrane expression that appears to be of physiological importance in neutrophils. However, RBL cells appear to be suitable to study apoptosis- or degranulation-induced PR3 membrane expression.

Regulation of myeloid proliferation and differentiation

As already mentioned, PR3 can be considered as a potential oncogene, as it can greatly enhance myeloid cell proliferation and can confer serum independence when overexpressed in myeloid cells [36]. We have reported that PR3 could enhance myeloid cell proliferation through p21^{cip1/waf1} cleavage. Accordingly, the PR3-resistant p21A45R mutant inhibited proliferation and promoted granulocytic differentiation. The present report demonstrates for the first time that the proliferative activity of PR3 depends on the presence of the hydrophobic patch, thus suggesting that PR3 membrane insertion might

play a role in PR3-proliferative activity, or this hydrophobic patch was essential in mediating essential protein-protein interactions for myeloid cell proliferation. Whether this observation could be useful for designing future therapies aiming at decreasing myeloid cell proliferation in leukemia remains to be evaluated.

AUTHORSHIP

C.K. and A.M. conceived of and performed experiments and helped to write the manuscript. J.G. performed experiments. E.H., T.B., and P.P. performed MD simulation experiments. N.R. conceived of molecular modeling experiments, analyzed data, and helped to write the manuscript. V.W-S. conceived of the project, planned and analyzed the experiments, and wrote the manuscript.

ACKNOWLEDGMENTS

Researchers were individually funded by fellowships from the Association "Vaincre La Mucoviscidose" (C.K. and J.G.), Société de Néphrologie (C.K.) and Société Française d'Hématologie (SFH; J.G.), and Institut National de la Santé et de la Recherche Médicale (INSERM; A.M. and V.W-S.). Funding for N.R., T.B., and E.H. was provided by the Functional Genomics (FUGE) in the Research Council of Norway and the Bergen Research Foundation and for V.W-S., by a grant from the National Research Agency [Agence Nationale pour la Recherche (ANR) Genopat]. Parallab (High Performance Computing Laboratory at the University of Bergen) and the Norwegian Metacenter for Computational Science (NOTUR) are thankfully acknowledged for provision of Central Processing Unit time to this project. The authors thank Valérie Gausson, Joyce Benchrutit, Clarisse Panterne, and Julie Mocek for their excellent technical assistance.

REFERENCES

1. Belaouaj, A., McCarthy, R., Baumann, M., Gao, Z., Ley, T. J., Abraham, S. N., Shapiro, S. D. (1998) Mice lacking neutrophil elastase reveal impaired host defense against gram negative bacterial sepsis. *Nat. Med.* **4**, 615–618.
2. Pham, C. T. (2006) Neutrophil serine proteases: specific regulators of inflammation. *Nat. Rev. Immunol.* **6**, 541–550.
3. Owen, C. A., Campbell, M. A., Sannes, P. L., Boukedes, S. S., Campbell, E. J. (1995) Cell surface-bound elastase and cathepsin G on human neutrophils: a novel, non-oxidative mechanism by which neutrophils focus and preserve catalytic activity of serine proteinases. *J. Cell Biol.* **131**, 775–789.
4. Campbell, E. J., Campbell, M. A., Owen, C. A. (2000) Bioactive proteinase 3 on the cell surface of human neutrophils: quantification, catalytic activity, and susceptibility to inhibition. *J. Immunol.* **165**, 3366–3374.
5. Campanelli, D., Melchior, M., Fu, Y., Nakata, M., Shuman, H., Nathan, C., Gabay, J. E. (1990) Cloning of cDNA for proteinase 3: a serine protease, antibiotic, and autoantigen from human neutrophils. *J. Exp. Med.* **172**, 1709–1715.
6. Witko-Sarsat, V., Cramer, E. M., Hieblot, C., Guichard, J., Nusbaum, P., Lopez, S., Lesavre, P., Halbwachs-Mecarelli, L. (1999) Presence of proteinase 3 in secretory vesicles: evidence of a novel, highly mobilizable intracellular pool distinct from azurophilic granules. *Blood* **94**, 2487–2496.
7. Hajjar, E., Broemstrup, T., Kantari, C., Witko-Sarsat, V., Reuter, N. (2010) Structures of human proteinase 3 and neutrophil elastase: so similar yet so different. *FEBS J.* **277**, 2238–2254.
8. Durant, S., Pederzoli, M., Lepelletier, Y., Canteloup, S., Nusbaum, P., Lesavre, P., Witko-Sarsat, V. (2004) Apoptosis-induced proteinase 3 membrane expression is independent from degranulation. *J. Leukoc. Biol.* **75**, 87–98.

9. Jennette, J. C., Xiao, H., Falk, R. J. (2006) Pathogenesis of vascular inflammation by anti-neutrophil cytoplasmic antibodies. *J. Am. Soc. Nephrol.* **17**, 1235–1242.
10. Morgan, M. D., Harper, L., Williams, J., Savage, C. (2006) Anti-neutrophil cytoplasm-associated glomerulonephritis. *J. Am. Soc. Nephrol.* **17**, 1224–1234.
11. Falk, R. J., Terrell, R. S., Charles, L. A., Jennette, J. C. (1990) Anti-neutrophil cytoplasmic autoantibodies induce neutrophils to degranulate and produce oxygen radicals in vitro. *Proc. Natl. Acad. Sci. USA* **87**, 4115–4119.
12. Csernok, E., Ernst, M., Schmitt, W., Bainton, D. F., Gross, W. L. (1994) Activated neutrophils express proteinase 3 on their plasma membrane in vitro and in vivo. *Clin. Exp. Immunol.* **95**, 244–250.
13. Kantari, C., Pederzoli-Ribeil, M., Amir-Moazami, O., Gausson-Dorey, V., Moura, I. C., Lecomte, M. C., Benhamou, M., Witko-Sarsat, V. (2007) Proteinase 3, the Wegener autoantigen, is externalized during neutrophil apoptosis: evidence for a functional association with phospholipid scramblase 1 and interference with macrophage phagocytosis. *Blood* **110**, 4086–4095.
14. Bories, D., Raynal, M. C., Solomon, D. H., Darzynkiewicz, Z., Cayre, Y. E. (1989) Down-regulation of a serine protease, myeloblastin, causes growth arrest and differentiation of promyelocytic leukemia cells. *Cell* **59**, 959–968.
15. Dengler, R., Munstermann, U., al-Batran, S., Hausner, I., Faderl, S., Nerl, C., Emmerich, B. (1995) Immunocytochemical and flow cytometric detection of proteinase 3 (myeloblastin) in normal and leukemic myeloid cells. *Br. J. Haematol.* **89**, 250–257.
16. Witko-Sarsat, V., Canteloup, S., Durant, S., Desdouets, C., Chabernaude, R., Lemarchand, P., Descamps-Latscha, B. (2002) Cleavage of p21waf1 by proteinase-3, a myeloid-specific serine protease, potentiates cell proliferation. *J. Biol. Chem.* **277**, 47338–47347.
17. Dublet, B., Ruello, A., Pederzoli, M., Hajjar, E., Courbebaisse, M., Canteloup, S., Reuter, N., Witko-Sarsat, V. (2005) Cleavage of p21/WAF1/CIP1 by proteinase 3 modulates differentiation of a monocytic cell line. Molecular analysis of the cleavage site. *J. Biol. Chem.* **280**, 30242–30253.
18. Goldmann, W. H., Niles, J. L., Arnaout, M. A. (1999) Interaction of purified human proteinase 3 (PR3) with reconstituted lipid bilayers. *Eur. J. Biochem.* **261**, 155–162.
19. Hajjar, E., Mihajlovic, M., Witko-Sarsat, V., Lazaridis, T., Reuter, N. (2008) Computational prediction of the binding site of proteinase 3 to the plasma membrane. *Proteins* **71**, 1655–1669.
20. Fujinaga, M., Chernaia, M. M., Halenbeck, R., Kothe, K., James, M. N. (1996) The crystal structure of PR3, a neutrophil serine proteinase antigen of Wegener's granulomatosis antibodies. *J. Mol. Biol.* **261**, 267–278.
21. Hajjar, E., Korkmaz, B., Gauthier, F., Brandsdal, B. O., Witko-Sarsat, V., Reuter, N. (2006) Inspection of the binding sites of proteinase 3 for the design of a highly specific substrate. *J. Med. Chem.* **49**, 1248–1260.
22. Pardo, J., Urban, C., Galvez, E. M., Ekert, P. G., Muller, U., Kwon-Chung, J., Lobigs, M., Mullbacher, A., Wallich, R., Borner, C., Simon, M. M. (2006) The mitochondrial protein Bak is pivotal for gliotoxin-induced apoptosis and a critical host factor of *Aspergillus fumigatus* virulence in mice. *J. Cell Biol.* **174**, 509–519.
23. Witko-Sarsat, V., Halbwachs-Mecarelli, L., Schuster, A., Nusbaum, P., Ueki, I., Canteloup, S., Lenoir, G., Descamps-Latscha, B., Nadel, J. A. (1999) Proteinase 3, a potent secretagogue in airways, is present in cystic fibrosis sputum. *Am. J. Respir. Cell Mol. Biol.* **20**, 729–736.
24. Broemstrup, T., Reuter, N. (2010) How does proteinase 3 interact with lipid bilayers? *Phys. Chem. Chem. Phys.* **12**, 7487–7496.
25. Hajjar, E., Korkmaz, B., Reuter, N. (2007) Differences in the substrate binding sites of murine and human proteinase 3 and neutrophil elastase. *FEBS Lett.* **581**, 5685–5690.
26. Mulgrew-Nesbitt, A., Diraviyam, K., Wang, J., Singh, S., Murray, P., Li, Z., Rogers, L., Mirkovic, N., Murray, D. (2006) The role of electrostatics in protein-membrane interactions. *Biochim. Biophys. Acta* **1761**, 812–826.
27. Witko-Sarsat, V., Reuter, N., Mouthon, L. (2010) Interaction of proteinase 3 with its associated partners: implications in the pathogenesis of Wegener's granulomatosis. *Curr. Opin. Rheumatol.* **22**, 1–7.
28. Hu, N., Westra, J., Kallenberg, C. G. M. (2009) Membrane-bound proteinase 3 and its receptors: relevance for the pathogenesis of Wegener's granulomatosis. *Autoimmun. Rev.* **8**, 510–514.
29. Halbwachs-Mecarelli, L., Bessou, G., Lesavre, P., Lopez, S., Witko-Sarsat, V. (1995) Bimodal distribution of proteinase 3 (PR3) surface expression reflects a constitutive heterogeneity in the polymorphonuclear neutrophil pool. *FEBS Lett.* **374**, 29–33.
30. Korkmaz, B., Jallat, J., Jourdan, M. L., Gauthier, A., Gauthier, F., Attucci, S. (2009) Catalytic activity and inhibition of Wegener antigen proteinase 3 on the cell surface of human polymorphonuclear neutrophils. *J. Biol. Chem.* **284**, 19896–19902.
31. Witko-Sarsat, V., Lesavre, P., Lopez, S., Bessou, G., Hieblot, C., Prum, B., Noel, L. H., Guillemin, L., Ravaut, P., Sermet-Gaudelus, I., Timsit, J., Grünfeld, J. P., Halbwachs-Mecarelli, L. (1999) A large subset of neutrophils expressing membrane proteinase 3 is a risk factor for vasculitis and rheumatoid arthritis. *J. Am. Soc. Nephrol.* **10**, 1224–1233.
32. Bauer, S., Abdgawad, M., Gunnarsson, L., Segelmark, M., Tapper, H., Hellmark, T. (2007) Proteinase 3 and CD177 are expressed on the plasma membrane of the same subset of neutrophils. *J. Leukoc. Biol.* **81**, 458–464.
33. Von Vietinghoff, S., Tunnemann, G., Eulenberg, C., Wellner, M., Cristina Cardoso, M., Luft, F. C., Kettritz, R. (2007) NB1 mediates surface expression of the ANCA antigen proteinase 3 on human neutrophils. *Blood* **109**, 4487–4493.
34. Korkmaz, B., Kuhl, A., Bayat, B., Santoso, S., Jenne, D. E. (2008) A hydrophobic patch on proteinase 3, the target of autoantibodies in Wegener granulomatosis, mediates membrane binding via NB1 receptors. *J. Biol. Chem.* **283**, 35976–35982.
35. Choi, M., Eulenberg, C., Rolle, S., von Kries, J. P., Luft, F. C., Kettritz, R. (2010) The use of small molecule high-throughput screening to identify inhibitors of the proteinase 3-NB1 interaction. *Clin. Exp. Immunol.* **161**, 389–396.
36. Lutz, P. G., Moog-Lutz, C., Coumau-Gatbois, E., Kobari, L., Di Gioia, Y., Cayre, Y. E. (2000) Myeloblastin is a granulocyte colony-stimulating factor-responsive gene conferring factor-independent growth to hematopoietic cells. *Proc. Natl. Acad. Sci. USA* **97**, 1601–1606.

KEY WORDS:

neutrophil • autoimmunity • vasculitis • leukemia • inflammation